

Edify 3D: Scalable High-Quality 3D Asset Generation

NVIDIA¹



Figure 1: Edify 3D is a model designed for high-quality 3D asset generation. With input text prompts and/or a reference image, our model can generate a wide range of detailed 3D assets, supporting applications such as video game design, extended reality, simulation, and more.

Abstract

We introduce Edify 3D, an advanced solution designed for high-quality 3D asset generation. Our method first synthesizes RGB and surface normal images of the described object at multiple viewpoints using a diffusion model. The multi-view observations are then used to reconstruct the shape, texture, and PBR materials of the object. Our method can generate high-quality 3D assets with detailed geometry, clean shape topologies, high-resolution textures, and materials within 2 minutes of runtime.

<https://research.nvidia.com/labs/dir/edify-3d>

1. Introduction

The creation of detailed digital 3D assets is essential for developing scenes, characters, and environments across various digital domains. This capability is invaluable to industries such as video game design, extended reality, film production, and simulation. For 3D content to be production-ready, it must meet industry standards, including precise mesh structures, high-resolution textures, and material maps. Consequently, producing such high-quality 3D content is often an exceedingly complex and time-intensive process. As demand for 3D digital experiences grows, the need for efficient, scalable solutions in 3D asset creation becomes increasingly crucial.

¹A detailed list of contributors and acknowledgments can be found in [App. A](#) of this paper.

Recently, many research works have investigated into training AI models for 3D asset generation (Lin et al., 2023). A significant challenge, however, is the limited availability of 3D assets suitable for model training. Creating 3D content requires specialized skills and expertise, making such assets much scarcer than other visual media like images and videos. This scarcity raises a key research question of how to design scalable models to generate high-quality 3D assets from such data efficiently.

Edify 3D is an advanced solution designed for high-quality 3D asset generation, addressing the above challenges while meeting industry standards. Our model generates high-quality 3D assets in under 2 minutes, providing detailed geometry, clean shape topologies, organized UV maps, textures up to 4K resolution, and physically-based rendering (PBR) materials. Compared to other text-to-3D approaches, Edify 3D consistently produces superior 3D shapes and textures, with notable improvements in both efficiency and scalability. This technical report provides a detailed description of Edify 3D.

Core capabilities. Edify 3D features the following capabilities:

- **Text-to-3D generation.** Given an input text description, Edify 3D generates a digital 3D asset with the aforementioned properties.
- **Image-to-3D generation.** Edify 3D can also create a 3D asset from a reference image of the object, automatically identifying the foreground object in the image.

Model design. The core technology of Edify 3D relies on two types of neural networks: diffusion models (Ho et al., 2020; Song and Ermon, 2019) and Transformers (Vaswani et al., 2017). Both architectures have demonstrated great scalability and success in improving generation quality as more training data becomes available. Following Li et al. (2024), we train the following models:

- **Multi-view diffusion models.** We train multiple diffusion models to synthesize the RGB appearance and surface normals of an object from multiple viewpoints (Shi et al., 2023). The input can be a text prompt, a reference image, or both.
- **Reconstruction model.** Using the synthesized multi-view RGB and surface normal images, a reconstruction model predicts the geometry, texture, and materials of the 3D shape. We employ a Transformer-based model (Hong et al., 2023) to predict a neural representation of the 3D object as latent tokens, followed by isosurface extraction and mesh processing.

The final output of Edify 3D is a 3D asset that includes the mesh geometry, texture map, and material map. Fig. 2 illustrates the overall pipeline of Edify 3D.

In this report, we provide:

- A detailed discussion of the design choices in the Edify 3D pipeline.
- An analysis of the scaling behaviors of model components and properties.
- An application of Edify 3D to scalable 3D scene generation from input text prompts.

2. Multi-View Diffusion Model

The process of creating multi-view images is similar to the design of video generation (Brooks et al., 2024; Chen et al., 2024). We finetune text-to-image models into pose-aware multi-view diffusion models by conditioning them with camera poses. The models take a text prompt and camera poses as input and synthesize the object’s appearance from different viewpoints. We train the following models:

1. A base multi-view diffusion model that synthesizes the RGB appearance conditioned on the input text prompt as well as the camera poses.
2. A multi-view ControlNet (Zhang et al., 2023) model that synthesizes the object’s surface normals, conditioned on both the multi-view RGB synthesis and the text prompt.

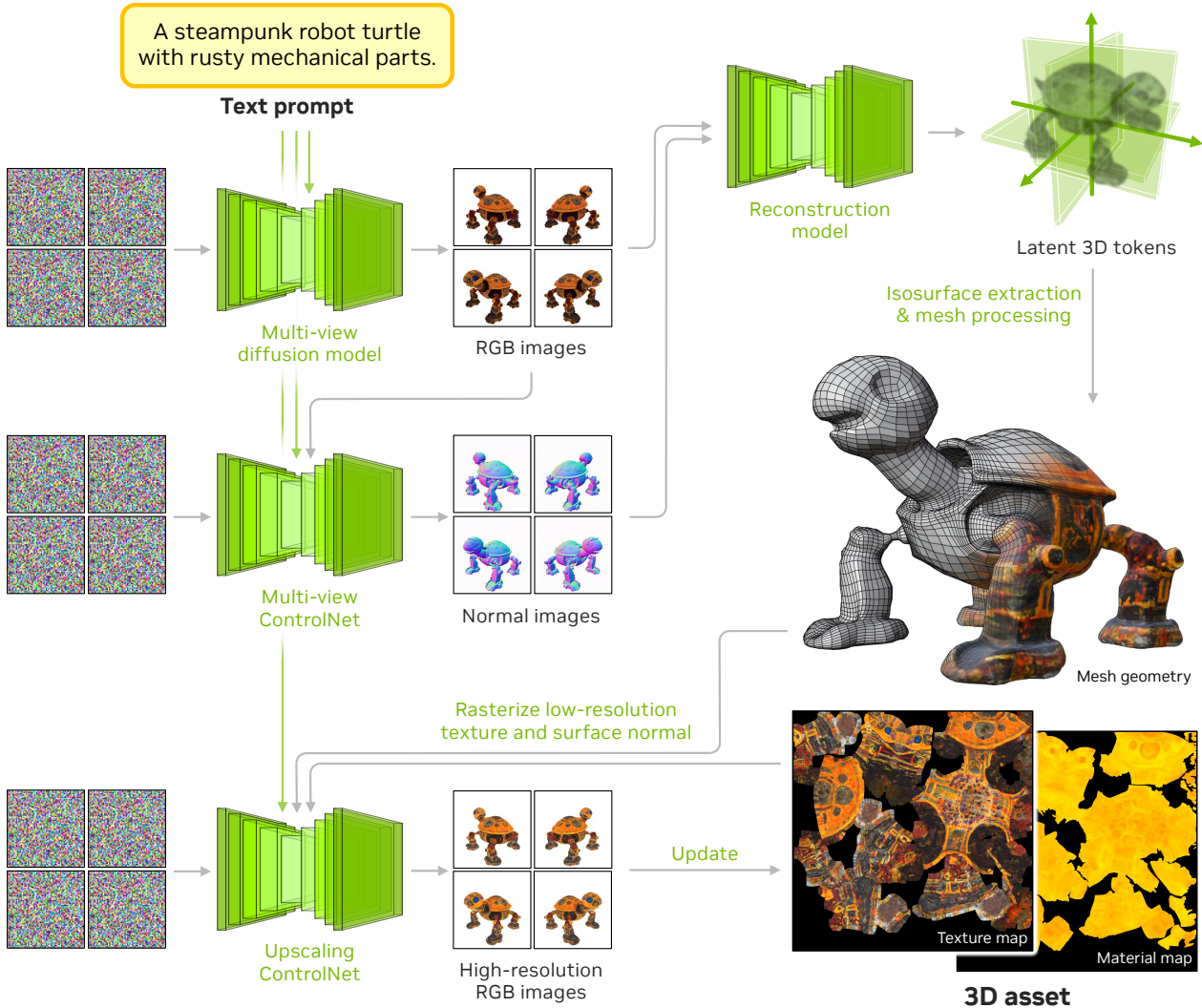


Figure 2: **Pipeline of Edify 3D.** Given a text description, a multi-view diffusion model synthesizes the RGB appearance of the described object. The generated multi-view RGB images are then used as a condition to synthesize surface normals using a multi-view ControlNet (Zhang et al., 2023). Next, a reconstruction model takes the multi-view RGB and normal images as input and predicts the neural 3D representation using a set of latent tokens. This is followed by isosurface extraction and subsequent mesh post-processing to obtain the mesh geometry. An upscaling ControlNet is used to increase the texture resolution, conditioning on mesh rasterizations to generate high-resolution multi-view RGB images, which are then back-projected onto the texture map.

3. A multi-view upscaling ControlNet that super-resolves the multi-view RGB images to a higher resolution, conditioned on the rasterized texture and surface normals of a given 3D mesh.

We use the Edify Image (NVIDIA et al., 2024) model as the base diffusion model architecture with a U-Net (Ronneberger et al., 2015) with 2.7 billion parameters, operating the diffusion in the pixel space. The ControlNet encoders are initialized using the weights from the U-Net. We extend the self-attention layer in the original text-to-image diffusion model with a new mechanism to attend across different views (Fig. 3), acting as a video diffusion model with the same weights. The camera poses (rotation and translation) are encoded through a lightweight MLP, which are subsequently added as the time embeddings to the video diffusion model architecture.

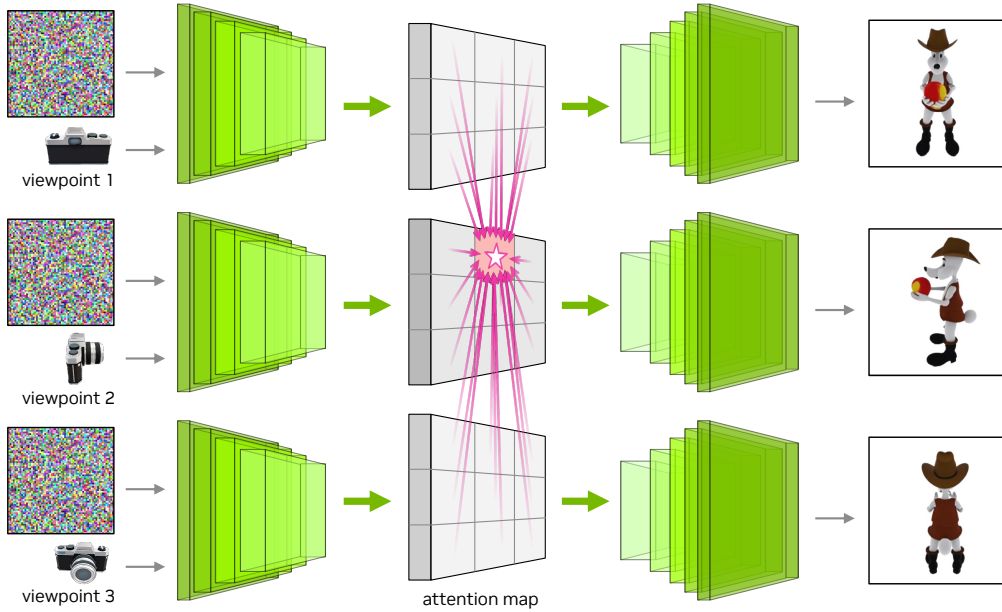


Figure 3: **Cross-view attention.** In standard diffusion models, each view is synthesized by the diffusion model independently. We extend the self-attention layer (yellow boxes) in our multi-view diffusion models to attend across other viewpoints using the same weights.

Training. We finetune the text-to-image models on renderings of 3D objects. During training, we jointly train on natural 2D images as well as 3D object renderings with randomly chosen numbers of views (1, 4, and 8). The diffusion models are trained using the x_0 parametrization for the loss, consistent with the approach used in base model training. For multi-view ControlNets, we train the base model with multi-view surface normal images first. Subsequently, we add a ControlNet encoder taking RGB images as input and train it while freezing the base model.

2.1. Ablation Studies

Scaling with respect to the number of viewpoints. During inference, we can sample an arbitrary number of views while maintaining good multi-view consistency, as shown in Fig. 4. Generating more views allows for broader coverage of the object’s regions in the multi-view images. As we later discuss in Sec. 3, the quality of the resulting 3D reconstruction is positively correlated to the number of multi-view observations (Furukawa and Ponce, 2009). Therefore, the ability of the multi-view diffusion model to synthesize denser viewpoints is critical to the final 3D generation quality.

Training across different numbers of viewpoints. During training, we sample 1, 4, or 8 views for each training object, assigning different sampling ratios for each number of views. While training with a varying number of views enables sampling an arbitrary number of views during inference, it is still preferable to match the training views to those expected during inference. This helps minimize the gap between training and inference performance. We compare between two models -- one trained primarily on 4-view images and one on 8-view images -- and sample 10-view images at the same viewpoints. As shown in Fig. 5, the model trained mostly with 8-view images produces more natural looking images with better multi-view consistency across views compared to that trained mostly with 4-view images.

3. Reconstruction Model

Extracting 3D structure from image observations is typically referred to as photogrammetry, which has been widely applied to many 3D reconstruction tasks (Li et al., 2023; Mildenhall et al., 2020; Wang et al.,

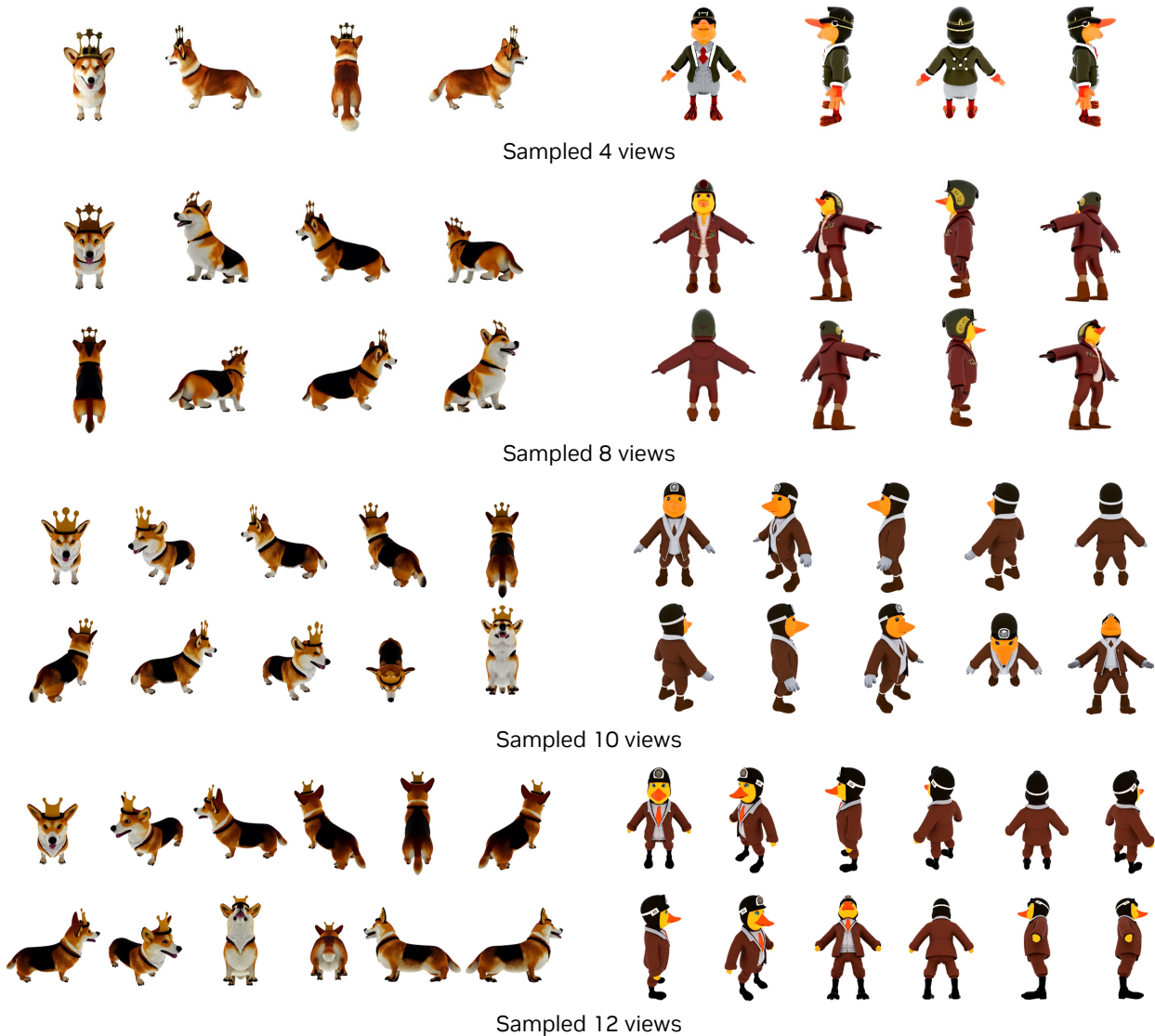


Figure 4: **Comparison of number of sampled views.** All images are sampled from the same model. Our multi-view diffusion model can synthesize object images with dense viewpoint coverage while maintaining good multi-view consistency, making it suitable for the downstream reconstruction model.

2021). We use a Transformer-based reconstruction model (Hong et al., 2023) to generate the 3D mesh geometry, texture map, and material map from multi-view images. We find that a Transformer-based model demonstrates strong generalization capabilities to unseen object images, including synthesized outputs from 2D multi-view diffusion models (Sec. 2).

We use a decoder-only Transformer model with a latent 3D representation as triplanes (Chan et al., 2023; Hong et al., 2023). The input RGB and normal images serve as conditioning for the reconstruction model, with cross-attention layers applied between triplane tokens and the input conditioning. The triplane tokens are processed through MLPs to predict neural fields for Signed Distance Functions (SDF) and PBR properties (Karis, 2013), which are used for SDF-based volume rendering (Yariv et al., 2021). The neural SDF is converted into a 3D mesh through isosurface extraction (Lorenson and Cline, 1998; Shen et al., 2023). The PBR properties are baked into texture and material maps via UV mapping, including albedo colors and material properties like roughness and metallic channels.



Figure 5: **Comparison of number of training views.** We compare two models trained primarily with different numbers of views (4 vs. 8), and sample images at the same 10 views at inference time. The model trained primarily on 8 views generates images with better multi-view consistency compared to the 4-view counterpart.

Training. We train our reconstruction model using large-scale imagery and 3D asset data. The model is supervised on depth, normal, mask, albedo, and material channels through SDF-based volume rendering, with outputs rendered from artist-generated meshes. Since surface normal computation is relatively expensive, we compute the normal only at the surface and supervise against the ground truth. We find that aligning the uncertainty of the SDF (Yariv et al., 2021) with the corresponding rendering resolution improves the visual quality of the final output. Additionally, we mask out object edges during loss computation to avoid noisy samples caused by aliasing. To smooth noisy gradients across samples, we apply exponential moving average (EMA) to aggregate the final reconstruction model weights.

Mesh post-processing. After obtaining the dense triangular 3D mesh from isosurface extraction, we post-process the mesh with the following steps:

1. Retopologize into a quadrilateral (quad) mesh with simplified geometry and adaptive topologies.
2. Generate the UV mapping based on the resulting quad mesh topology.
3. Bake the albedo and material neural fields into a texture map and material map, respectively.

These post-processing steps make the resulting mesh more suitable for further editing, essential for artistic and design-oriented downstream applications.

3.1. Ablation Studies

We study the scaling properties of the reconstruction model in the following aspects: (a) the number of input images and (b) the tokens representing the shapes.

Experimental setup. For validation, we randomly select 78 shapes from a held-out dataset. We report the LPIPS (Zhang et al., 2018) score on the albedo prediction to quantify the base texture reconstruction performance. For material prediction accuracy, we use the L_2 error on the roughness and metallic values. We also use the L_2 error between the ground-truth and predicted depths as a proxy for evaluating the geometry accuracy of the reconstructed shapes. The camera poses used for input and output are fixed at an elevation of 20° , pointing towards the origin (Fig. 6).

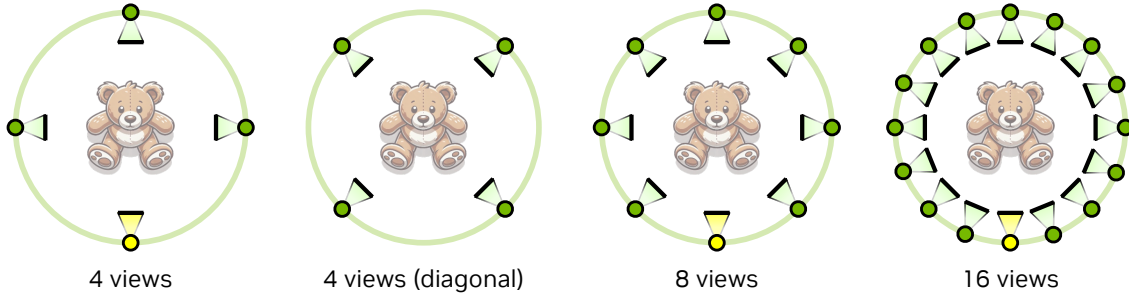


Figure 6: **Camera pose sets for scaling reconstruction.** The camera poses are set at various azimuth angles and a fixed elevation of 20° . The camera in yellow indicates the “frontal” pose with respect to a canonicalized coordinate system. In each setup, the cameras are uniformly distributed around a circus at a fixed radius looking towards the origin. The “4 views (diagonal)” represents the same 4-view pose set but with a 45° offset, resulting in the cameras looking at the object region from diagonal angles.

Albedo LPIPS error					Material L_2 error					Depth L_2 error				
Input views	Validation views				Input views	Validation views				Input views	Validation views			
	4	4 (diag.)	8	16		4	4 (diag.)	8	16		4	4 (diag.)	8	16
4	0.0732	0.0791	0.0762	0.0768	4	0.0015	0.0020	0.0017	0.0018	4	0.0689	0.0751	0.0720	0.0722
4 (diag.)	0.0802	0.0756	0.0779	0.0783	4 (diag.)	0.0024	0.0019	0.0022	0.0022	4 (diag.)	0.0704	0.0683	0.0694	0.0696
8	0.0691	0.0698	0.0695	0.0699	8	0.0013	0.0012	0.0013	0.0013	8	0.0626	0.0641	0.0633	0.0633
16	0.0687	0.0689	0.0688	0.0687	16	0.0012	0.0013	0.0013	0.0013	16	0.0613	0.0626	0.0619	0.0616

Table 1: **Comparison of the number of input views.** The diagonal cells indicate the cases where the input views match the validation views. The quality improves (error decreases) as the number of input views increases, demonstrating the scalability of our reconstruction model.

Scaling with respect to the number of viewpoints. We find that our reconstruction model consistently recovers the input views more accurately than novel views. The model scales well with respect to the number of viewpoints, i.e., its performance improves as more information is provided. We demonstrate this with various combinations of input and output camera views, as shown in Fig. 6.

We present the quantitative results in Tab. 1. The diagonal entries of the table are highlighted, as they represent cases where the inputs and outputs are identical. These diagonal entries often show the best results in each row, indicating that the model reproduces the input views most accurately. Additionally, the results consistently improve as the number of input views increases from 4 to 16. This suggests that the reconstruction model benefits from the additional input information.

Motivated by the model’s scaling with the number of viewpoints, we further investigate whether the number of training views affects reconstruction quality. We evaluate the model using a fixed 8-view setup, where the model is trained with 4, 6, 8, and 10 views. The results are shown in Fig. 7a. Although stochastic sampling of camera poses provides diverse viewpoints during training, the reconstruction quality continues to improve as the number of training views in the same training step increases.

Scaling with respect to compute. We study the impact of the compute requirements of the reconstruction model without changing the model size (i.e., the number of model parameters). For this analysis, we scale down the triplane token sizes in the self-attention and cross-attention blocks to reduce computation. Note that this adjustment does not alter the number of model parameters. We observe from Fig. 7b that as the number of tokens increases, the results improve proportionally with the available compute.

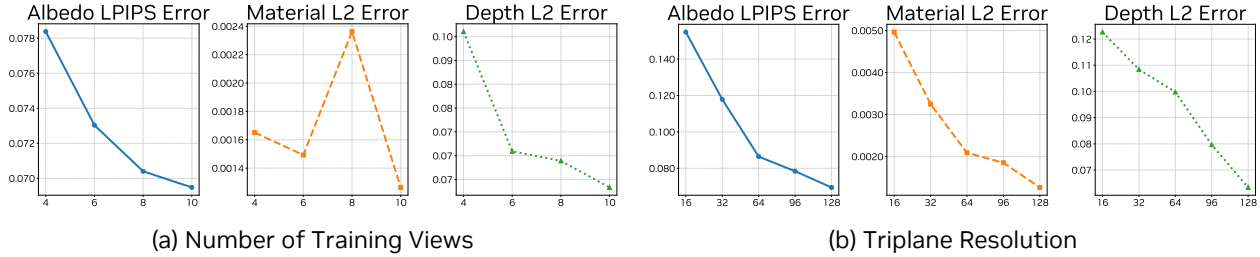


Figure 7: (a) **Comparison of the number of training views.** The reconstruction model continues to improve as the number of training views increases. (b) **Comparison of the number of tokens.** With a fixed number of parameters, the model requires more compute with larger number of tokens. Note that the self-attention FLOPs increase quadratically with the triplane resolution. The quality consistently scales with the amount of compute.

4. Data Processing

Edify 3D is trained on a combination of non-public large-scale imagery, pre-rendered multi-view images, and 3D shape datasets. We focus on pre-processing 3D shape data in this section. The raw 3D data undergo several preprocessing steps to achieve the quality and format required for model training.

Format conversion. The first step of the data processing pipeline involves converting all 3D shapes into a unified format. We triangulate the meshes, pack all texture files, and convert the materials into metallic-roughness format. We discard shapes with corrupted textures or materials. This process results in a collection of 3D shapes that can be rendered as intended by the original creators.

Quality filtering. We filter out non-object-centric data from the large-scale 3D datasets. We render the shapes from multiple viewpoints and use AI classifiers to remove partial 3D scans, large scenes, shape collages, and shapes containing auxiliary structures such as backdrops and ground planes. To ensure quality, this process is conducted through multiple rounds of active learning, with human experts continuously curating challenging examples to refine the AI classifier. Additionally, we apply rule-based filtering to remove shapes with obvious issues, such as those that are excessively thin or lack texture.

Canonical pose alignment. We align our training shapes to their canonical poses to reduce potential ambiguity when training the model. Pose alignment is also achieved via active learning. We manually curate a small number of examples, train a pose predictor, look for hard examples in the full dataset, and repeat the process. Defining the canonical pose is also critical. While many objects such as cars, animals, and shoes already have natural canonical poses, other shapes may lack a clear front side, in which case we define the functional part as the front and prioritize maintaining left-right symmetry.

PBR rendering. To render the 3D data into images for the diffusion and reconstruction models, we use an in-house path tracer for photorealistic rendering. We employ a diverse set of sampling techniques for the camera parameters. Half of the images are rendered from fixed elevation angles with consistent intrinsic parameters, while the remaining images are rendered using random camera poses and intrinsics. As a constraint, we maintain roughly consistent object sizes within the rendered images. This approach accommodates both text-to-3D use cases (where there is full control over the camera parameters) and image-to-3D use cases (where the reference image may come from a wide range of camera intrinsics).

AI captions. To caption the 3D shapes, we render one image per shape and use a vision-language model (VLM) to generate both long and short captions for the image. To enhance the comprehensiveness of captions, we also provide the metadata of the shape (e.g. title, description, category tree) to the VLM.

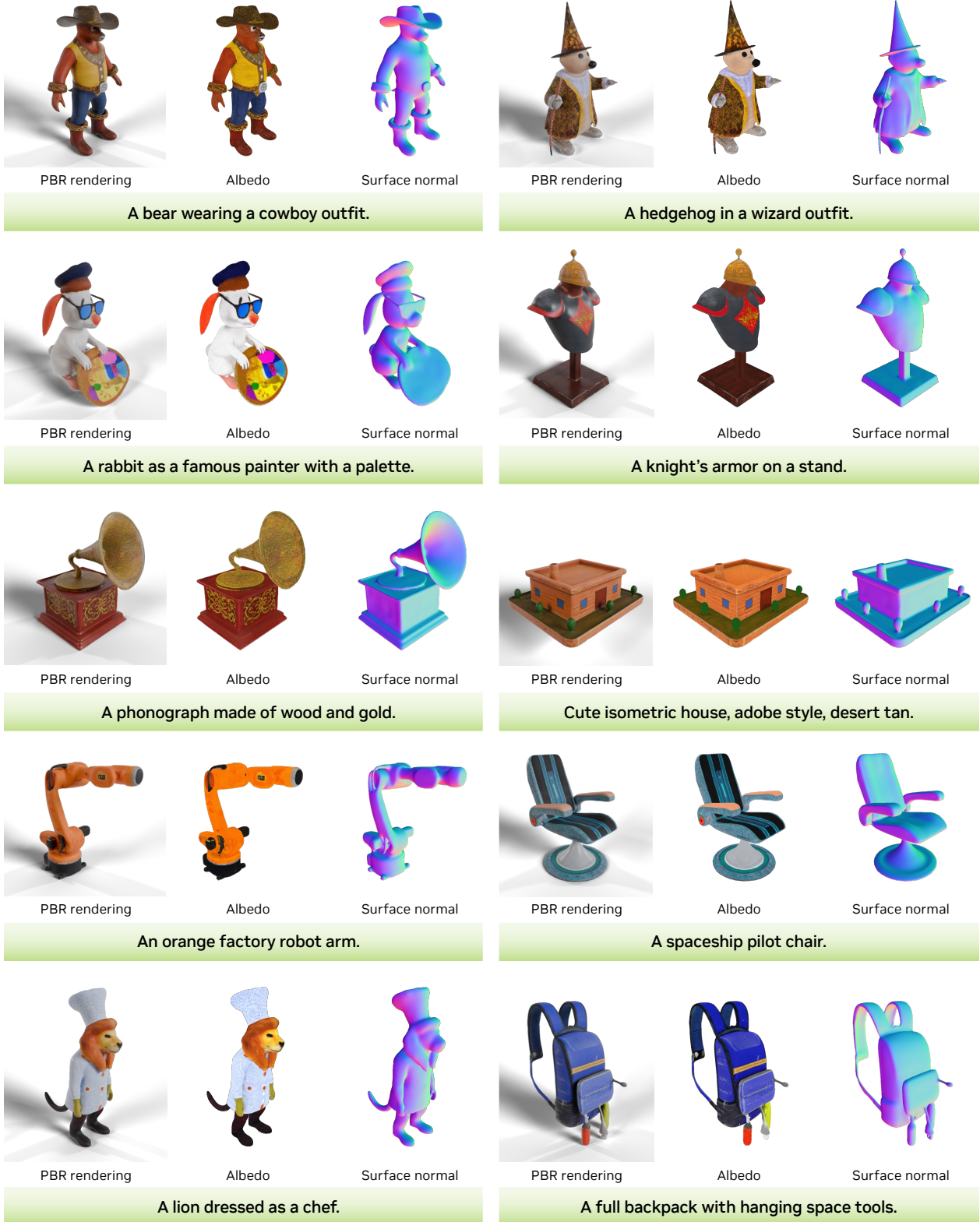


Figure 8: **Text-to-3D generation results.** We include the input text prompts as well as renderings and surface normals of generated assets. The generated 3D meshes include detailed geometry and sharp textures with well-decomposed albedo colors, making them suitable for various downstream editing and rendering applications.

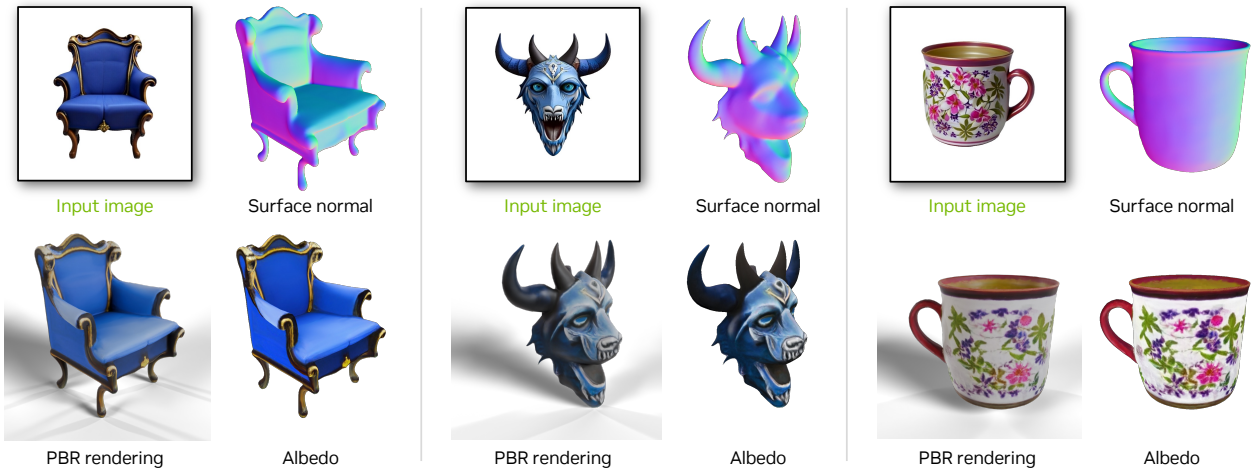


Figure 9: **Image-to-3D generation results.** We visualize the input reference images as well as renderings and surface normals of generated assets. Edify 3D can faithfully recover the underlying 3D structures of the reference object while also being able to hallucinate detailed textures in unseen surface regions (e.g., the backside of the cup).



Figure 10: **Quad mesh topologies.** Edify 3D generates assets in the form of quad meshes with clean topologies, making it suitable for downstream editing workflows. We visualize the quad mesh topologies of the generated assets with their PBR renderings side-by-side.

5. Results

We showcase text-to-3D generation results from Edify 3D in Fig. 8 and image-to-3D generation in Fig. 9. The generated meshes include detailed geometry and sharp textures, with well-decomposed albedo colors that represent the surface's base color. For image-to-3D generation, Edify 3D not only accurately recovers the underlying 3D structures of the reference object, but it also can generate detailed textures in regions of the surface not directly observed in the input image.

The assets generated by Edify 3D come in the form of quad meshes with well-organized topologies, as visualized in Fig. 10. These structured meshes allow for easier manipulation and precise adjustments,

making them well-suited for various downstream editing tasks and rendering applications. This enables seamless integration into 3D workflows that require visual fidelity and flexibility.

6. Related Work

3D asset generation. The challenge of 3D asset generation is often addressed by training models on 3D datasets (Gupta et al., 2023; Jun and Nichol, 2023; Nichol et al., 2022; Zeng et al., 2022), but the scarcity of these datasets limits the ability to generalize. To overcome this, recent methods have shifted towards using models trained on large-scale image and video datasets. Score Distillation Sampling (SDS) (Poole et al., 2023) has been adopted in earlier methods (Huang et al., 2023; Lin et al., 2023; Sun et al., 2024; Tang et al., 2023; Wang et al., 2023, 2024; Yi et al., 2023; Zhu and Zhuang, 2023) and extended to image-conditioned 3D generative models (Liu et al., 2023; Long et al., 2024; Qian et al., 2024; Tang et al., 2023; Wang and Shi, 2023; Yu et al., 2023). However, they often experience slow processing (Lorraine et al., 2023; Xie et al., 2024) and are susceptible to issues such as the Janus face issue (Shi et al., 2023). To improve performance, newer techniques integrate multi-view image generative models, focusing on producing multiple consistent views that can be reconstructed into 3D models (Chan et al., 2023; Chen et al., 2024; Gao et al., 2024; Höllein et al., 2024; Liu et al., 2024; Shi et al., 2023; Tang et al., 2024; Weng et al., 2023; Yang et al., 2024). However, maintaining consistency across these views remains a challenge, leading to the development of methods that enhance reconstruction robustness from limited views (Li et al., 2024; Liu et al., 2024).

3D reconstruction from multi-view images. 3D asset generation from limited views often involves 3D reconstruction techniques, often with differentiable rendering, that can utilize various 3D representations such as Neural Radiance Fields (NeRF) (Mildenhall et al., 2020). Meshes are the most commonly used format in industrial 3D engines, yet reconstructing high-quality meshes from multi-view images is challenging. Traditional photogrammetry pipelines, including structure from motion (SfM) (Agarwal et al., 2011; Schönberger and Frahm, 2016; Snavely et al., 2006), multi-view stereo (MVS) (Furukawa and Ponce, 2009; Schönberger et al., 2016), and surface extraction (Kazhdan et al., 2006; Lorensen and Cline, 1998; Shen et al., 2021, 2023), are costly and time-consuming, often yielding low-quality results. While NeRF-based neural rendering methods can achieve high-quality 3D reconstructions (Guédon and Lepetit, 2024; Huang et al., 2024; Kerbl et al., 2023; Li et al., 2023; Wang et al., 2021; Yariv et al., 2021), they require dense images and extensive optimization, and converting radiance fields into meshes can lead to suboptimal results. To address these limitations, Transformer-based (Vaswani et al., 2017) models further improve 3D NeRF reconstruction from sparse views by learning a feed-forward prior (Hong et al., 2023).

Texture and material generation. Earlier approaches targeting 3D texture generation given a 3D shape include CLIP (Radford et al., 2021) for text alignment (Michel et al., 2022; Mohammad Khalid et al., 2022) and SDS loss optimization (Poole et al., 2023). To improve 3D awareness, some text-to-3D methods combine texture inpainting with depth-conditioned diffusion (Chen et al., 2023), albeit slower and more artifact-prone. To enhance consistency, other techniques alternate diffusion with reprojection (Cao et al., 2023) or generate multiple textured views simultaneously (Deng et al., 2024), though at a higher computational cost. To further enhance realism, some methods have enabled multi-view PBR modeling (Boss et al., 2022; Zhang et al., 2021) to extend support for generating material properties (Chen et al., 2023; Qiu et al., 2024; Xu et al., 2023).

7. Application: 3D Scene Generation

In this section, we demonstrate an application of our Edify 3D model to scalable 3D scene generation (Bahmani et al., 2023). High-quality, large-scale 3D scenes are pivotal for content creation and training robust embodied AI agents. However, existing scene creation mostly depends on 3D scans

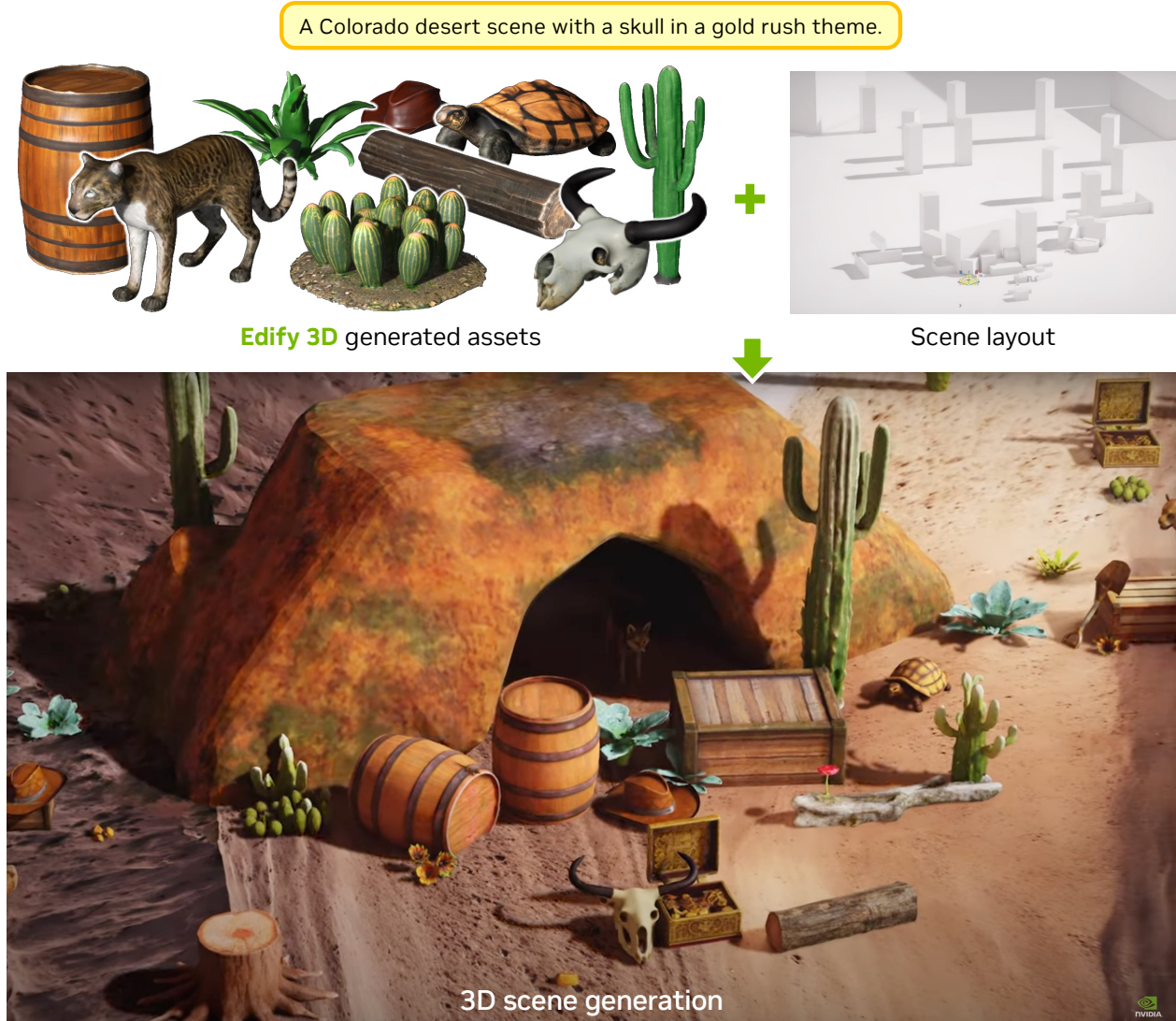


Figure 11: The high-quality 3D assets generated by Edify 3D can be extended to 3D scene generation combined with a given scene layout, which can be generated by an LLM. This enables the generated 3D scene to be readily rendered at high quality while being editable for various downstream applications.

with costly human annotations (Dai et al., 2017) or direct scene modeling (Bautista et al., 2022; Chen et al., 2023; Fridman et al., 2024), which largely limits the scalability.

With Edify 3D as the 3D asset generation API, we can design a scalable system to generate 3D scenes from only an input text prompt (Lin et al., 2024). The system generates the *scene layout* of 3D objects with Large Language Models (LLM) (OpenAI et al., 2023), which specifies the positions and sizes of 3D objects². As a result, the system can generate a realistic and complex 3D scene that coherently aligns with the text prompt describing the whole scene.

We show an example result of 3D scene generation in Fig. 11. The generated assets from Edify 3D include detailed geometry and textures, forming a scene composition together with a generated scene layout. Since all the 3D assets are created individually, the generated 3D scene is naturally editable for various specialized applications, such as artist creation, 3D designs, or embodied AI simulations.

²We refer the readers to Lin et al. (2024) for details on layout generation with LLMs.

8. Conclusion

In this technical report, we present Edify 3D, a solution designed for high-quality 3D asset generation. We introduce the Edify 3D models, analyze the scaling laws of each model, and describe the data curation pipeline. Additionally, we explore the application of Edify 3D to scalable 3D scene generation. We are committed to advancing and developing new automation tools for 3D asset generation, making 3D content creation more accessible to everyone.

A. Contributors and Acknowledgements

A.1. Core Contributors

System design: Chen-Hsuan Lin, Xiaohui Zeng, Zhaoshuo Li, Zekun Hao, Ming-Yu Liu, Tsung-Yi Lin.

Multi-view diffusion model: Xiaohui Zeng, Qinsheng Zhang, Ming-Yu Liu, Tsung-Yi Lin.

Reconstruction model: Zhaoshuo Li, Chen-Hsuan Lin, Zekun Hao, Yen-Chen Lin, Ming-Yu Liu, Tsung-Yi Lin.

3D data processing: Zekun Hao, Fangyin Wei, Yin Cui, Yunhao Ge, Yifan Ding, Donglai Xiang, Qianli Ma, Jacob Munkberg, Jon Hasselgren, Chen-Hsuan Lin, Tsung-Yi Lin.

Mesh post-processing: Donglai Xiang, Qianli Ma, J.P. Lewis, Zekun Hao, Zhaoshuo Li, Fangyin Wei, Xiaohui Zeng, Jingyi Jin, Chen-Hsuan Lin, Tsung-Yi Lin.

Evaluation: Jingyi Jin, Xiaohui Zeng, Zhaoshuo Li, Qianli Ma, Yen-Chen Lin, Chen-Hsuan Lin, Tsung-Yi Lin.

A.2. Contributors

Maciej Bala, Jacob Huffman, Alice Luo, Stella Shi, Jiashu Xu.

A.3. Acknowledgements

We thank Lars Bishop, Sanja Fidler, Jun Gao, Jinwei Gu, Aaron Lefohn, Arun Mallya, Hanzi Mao, Seungjun Nah, Fitsum Reda, David Romero Guzman, Rohan Sawhney, Nicholas Sharp, Tianchang Shen, Peter Shipkov, Towaki Takikawa, Heng Wang, and Martin Watt for useful research discussions and prototyping. We also thank Dane Aconfora, Yazdan Aghaghiri, Margaret Albrecht, Arslan Ali, Sivakumar Arayandi Thottakara, Amelia Barton, Lucas Brown, Matt Catrett, Douglas Chang, Steve Chappell, Gerardo Delgado Cabrera, John Dickinson, Amol Fasale, Daniela Flamm Jackson, Sandra Froehlich, Devika Ghaisas, Yugi Guvvala, Brett Hamilton, Mohammad Harrim, Nathan Horrocks, Akan Huang, Sophia Huang, Pooya Jannaty, Pranjali Joshi, Tobias Lasser, Gabriele Leone, Aaron Licata, Ashlee Martino-Tarr, Alexandre Milesi, Amanda Moran, Pawel Morkisz, Andrew Morse, Jashojit Mukherjee, Brad Nemire, Dade Orgeron, David Page, Mitesh Patel, Jason Paul, Joel Pennington, Lyne Tchapmi, Jibin Varghese, Thomas Volk, Raju Wagwani, Herb Woodruff, and Josh Young for feedback and support.

References

- [1] Sameer Agarwal, Yasutaka Furukawa, Noah Snavely, Ian Simon, Brian Curless, Steven M Seitz, and Richard Szeliski. Building rome in a day. *Communications of the ACM*, 2011. 11
- [2] Sherwin Bahmani, Jeong Joon Park, Despoina Paschalidou, Xingguang Yan, Gordon Wetzstein, Leonidas Guibas, and Andrea Tagliasacchi. Cc3d: Layout-conditioned generation of compositional 3d scenes. In *ICCV*, 2023. 11
- [3] Miguel Angel Bautista, Pengsheng Guo, Samira Abnar, Walter Talbott, Alexander Toshev, Zhuoyuan Chen, Laurent Dinh, Shuangfei Zhai, Hanlin Goh, Daniel Ulbricht, et al. Gaudi: A neural architect for immersive 3d scene generation. In *NeurIPS*, 2022. 12
- [4] Mark Boss, Andreas Engelhardt, Abhishek Kar, Yuanzhen Li, Deqing Sun, Jonathan Barron, Hendrik Lensch, and Varun Jampani. Samurai: Shape and material from unconstrained real-world arbitrary image collections. In *NeurIPS*, 2022. 11
- [5] Tim Brooks, Bill Peebles, Connor Holmes, Will DePue, Yufei Guo, Li Jing, David Schnurr, Joe Taylor, Troy Luhman, Eric Luhman, Clarence Ng, Ricky Wang, and Aditya Ramesh. Video generation models as world simulators. 2024. URL <https://openai.com/research/video-generation-models-as-world-simulators>. 2
- [6] Tianshi Cao, Karsten Kreis, Sanja Fidler, Nicholas Sharp, and Kangxue Yin. Textfusion: Synthesizing 3d textures with text-guided image diffusion models. In *ICCV*, 2023. 11
- [7] Eric R Chan, Koki Nagano, Matthew A Chan, Alexander W Bergman, Jeong Joon Park, Axel Levy, Miika Aittala, Shalini De Mello, Tero Karras, and Gordon Wetzstein. Generative novel view synthesis with 3d-aware diffusion models. In *ICCV*, 2023. 5, 11
- [8] Dave Zhenyu Chen, Yawar Siddiqui, Hsin-Ying Lee, Sergey Tulyakov, and Matthias Nießner. Text2tex: Text-driven texture synthesis via diffusion models. In *ICCV*, 2023. 11
- [9] Rui Chen, Yongwei Chen, Ningxin Jiao, and Kui Jia. Fantasia3d: Disentangling geometry and appearance for high-quality text-to-3d content creation. In *ICCV*, 2023. 11
- [10] Zhaoxi Chen, Guangcong Wang, and Ziwei Liu. Scenedreamer: Unbounded 3d scene generation from 2d image collections. *TPAMI*, 2023. 12
- [11] Zilong Chen, Yikai Wang, Feng Wang, Zhengyi Wang, and Huaping Liu. V3d: Video diffusion models are effective 3d generators. *arXiv preprint arXiv:2403.06738*, 2024. 2, 11
- [12] Angela Dai, Angel X Chang, Manolis Savva, Maciej Halber, Thomas Funkhouser, and Matthias Nießner. Scannet: Richly-annotated 3d reconstructions of indoor scenes. In *CVPR*, 2017. 12
- [13] Kangle Deng, Timothy Omernick, Alexander Weiss, Deva Ramanan, Jun-Yan Zhu, Tinghui Zhou, and Maneesh Agrawala. Flashtex: Fast relightable mesh texturing with lightcontrolnet. *arXiv preprint arXiv:2402.13251*, 2024. 11
- [14] Rafail Fridman, Amit Abecasis, Yoni Kasten, and Tali Dekel. Scenescape: Text-driven consistent scene generation. In *NeurIPS*, 2024. 12
- [15] Yasutaka Furukawa and Jean Ponce. Accurate, dense, and robust multiview stereopsis. *TPAMI*, 2009. 4, 11
- [16] Ruiqi Gao, Aleksander Holynski, Philipp Henzler, Arthur Brussee, Ricardo Martin-Brualla, Pratul Srinivasan, Jonathan T Barron, and Ben Poole. Cat3d: Create anything in 3d with multi-view diffusion models. *arXiv preprint arXiv:2405.10314*, 2024. 11

- [17] Antoine Guédon and Vincent Lepetit. Sugar: Surface-aligned gaussian splatting for efficient 3d mesh reconstruction and high-quality mesh rendering. In *CVPR*, 2024. 11
- [18] Anchit Gupta, Wenhan Xiong, Yixin Nie, Ian Jones, and Barlas Oğuz. 3dgen: Triplane latent diffusion for textured mesh generation. *arXiv preprint arXiv:2303.05371*, 2023. 11
- [19] Jonathan Ho, Ajay Jain, and Pieter Abbeel. Denoising diffusion probabilistic models. In *NeurIPS*, 2020. 2
- [20] Lukas Höllein, Norman Müller, David Novotny, Hung-Yu Tseng, Christian Richardt, Michael Zollhöfer, Matthias Nießner, et al. Viewdiff: 3d-consistent image generation with text-to-image models. In *CVPR*, 2024. 11
- [21] Yicong Hong, Kai Zhang, Jiuxiang Gu, Sai Bi, Yang Zhou, Difan Liu, Feng Liu, Kalyan Sunkavalli, Trung Bui, and Hao Tan. Lrm: Large reconstruction model for single image to 3d. *arXiv preprint arXiv:2311.04400*, 2023. 2, 5, 11
- [22] Binbin Huang, Zehao Yu, Anpei Chen, Andreas Geiger, and Shenghua Gao. 2d gaussian splatting for geometrically accurate radiance fields. In *SIGGRAPH*, 2024. 11
- [23] Yukun Huang, Jianan Wang, Yukai Shi, Xianbiao Qi, Zheng-Jun Zha, and Lei Zhang. Dreamtime: An improved optimization strategy for text-to-3d content creation. *arXiv preprint arXiv:2306.12422*, 2023. 11
- [24] Heewoo Jun and Alex Nichol. Shap-e: Generating conditional 3d implicit functions. *arXiv preprint arXiv:2305.02463*, 2023. 11
- [25] Brian Karis. Real shading in unreal engine 4. In *Physically Based Shading Theory Practice*, 2013. 5
- [26] Michael Kazhdan, Matthew Bolitho, and Hugues Hoppe. Poisson surface reconstruction. In *SGP*, 2006. 11
- [27] Bernhard Kerbl, Georgios Kopanas, Thomas Leimkühler, and George Drettakis. 3d gaussian splatting for real-time radiance field rendering. *ACM Transactions on Graphics (TOG)*, 2023. 11
- [28] Jiahao Li, Hao Tan, Kai Zhang, Zexiang Xu, Fujun Luan, Yinghao Xu, Yicong Hong, Kalyan Sunkavalli, Greg Shakhnarovich, and Sai Bi. Instant3d: Fast text-to-3d with sparse-view generation and large reconstruction model. In *ICLR*, 2024. 2, 11
- [29] Zhaoshuo Li, Thomas Müller, Alex Evans, Russell H Taylor, Mathias Unberath, Ming-Yu Liu, and Chen-Hsuan Lin. Neuralangelo: High-fidelity neural surface reconstruction. In *CVPR*, 2023. 4, 11
- [30] Chen-Hsuan Lin, Jun Gao, Luming Tang, Towaki Takikawa, Xiaohui Zeng, Xun Huang, Karsten Kreis, Sanja Fidler, Ming-Yu Liu, and Tsung-Yi Lin. Magic3d: High-resolution text-to-3d content creation. In *CVPR*, 2023. 2, 11
- [31] Tsung-Yi Lin, Chen-Hsuan Lin, Yin Cui, Yunhao Ge, Seungjun Nah, Arun Mallya, Zekun Hao, Yifan Ding, Hanzi Mao, Zhaoshuo Li, et al. Genusd: 3d scene generation made easy. In *ACM SIGGRAPH 2024 Real-Time Live!* 2024. 12
- [32] Minghua Liu, Ruoxi Shi, Linghao Chen, Zhuoyang Zhang, Chao Xu, Xinyue Wei, Hansheng Chen, Chong Zeng, Jiayuan Gu, and Hao Su. One-2-3-45++: Fast single image to 3d objects with consistent multi-view generation and 3d diffusion. In *CVPR*, 2024. 11
- [33] Minghua Liu, Chao Xu, Haian Jin, Linghao Chen, Mukund Varma T, Zexiang Xu, and Hao Su. One-2-3-45: Any single image to 3d mesh in 45 seconds without per-shape optimization. In *NeurIPS*, 2024. 11

-
- [34] Ruoshi Liu, Rundi Wu, Basile Van Hoorick, Pavel Tokmakov, Sergey Zakharov, and Carl Vondrick. Zero-1-to-3: Zero-shot one image to 3d object. In *ICCV*, 2023. 11
- [35] Xiaoxiao Long, Yuan-Chen Guo, Cheng Lin, Yuan Liu, Zhiyang Dou, Lingjie Liu, Yuexin Ma, Song-Hai Zhang, Marc Habermann, Christian Theobalt, et al. Wonder3d: Single image to 3d using cross-domain diffusion. In *CVPR*, 2024. 11
- [36] William E Lorensen and Harvey E Cline. Marching cubes: A high resolution 3d surface construction algorithm. In *Seminal graphics: pioneering efforts that shaped the field*. 1998. 5, 11
- [37] Jonathan Lorraine, Kevin Xie, Xiaohui Zeng, Chen-Hsuan Lin, Towaki Takikawa, Nicholas Sharp, Tsung-Yi Lin, Ming-Yu Liu, Sanja Fidler, and James Lucas. Att3d: Amortized text-to-3d object synthesis. In *ICCV*, 2023. 11
- [38] Oscar Michel, Roi Bar-On, Richard Liu, Sagie Benaim, and Rana Hanocka. Text2mesh: Text-driven neural stylization for meshes. In *CVPR*, 2022. 11
- [39] Ben Mildenhall, Pratul P. Srinivasan, Matthew Tancik, Jonathan T. Barron, Ravi Ramamoorthi, and Ren Ng. Nerf: Representing scenes as neural radiance fields for view synthesis. In *ECCV*, 2020. 4, 11
- [40] Nasir Mohammad Khalid, Tianhao Xie, Eugene Belilovsky, and Tiberiu Popa. Clip-mesh: Generating textured meshes from text using pretrained image-text models. In *SIGGRAPH Asia*, 2022. 11
- [41] Alex Nichol, Heewoo Jun, Prafulla Dhariwal, Pamela Mishkin, and Mark Chen. Point-e: A system for generating 3d point clouds from complex prompts. *arXiv preprint arXiv:2212.08751*, 2022. 11
- [42] NVIDIA, Yuval Atzmon, Maciej Bala, Yogesh Balaji, Tiffany Cai, Yin Cui, Jiaojiao Fan, Yunhao Ge, Siddharth Gururani, Jacob Huffman, Ronald Isaac, Pooya Jannaty, Tero Karras, Grace Lam, J. P. Lewis, Aaron Licata, Yen-Chen Lin, Ming-Yu Liu, Qianli Ma, Arun Mallya, Ashlee Martino-Tarr, Doug Mendez, Seungjun Nah, Chris Pruet, Fitsum Reda, Jiaming Song, Ting-Chun Wang, Fangyin Wei, Xiaohui Zeng, Yu Zeng, and Qinsheng Zhang. Edify image: High-quality image generation with pixel space laplacian diffusion models. 2024. 3
- [43] OpenAI, Josh Achiam, Steven Adler, Sandhini Agarwal, Lama Ahmad, Ilge Akkaya, Florencia Leoni Aleman, Diogo Almeida, Janko Altmenschmidt, Sam Altman, Shyamal Anadkat, et al. Gpt-4 technical report. *arXiv preprint arXiv:2303.08774*, 2023. 12
- [44] Ben Poole, Ajay Jain, Jonathan T Barron, and Ben Mildenhall. Dreamfusion: Text-to-3d using 2d diffusion. In *ICLR*, 2023. 11
- [45] Guocheng Qian, Jinjie Mai, Abdullah Hamdi, Jian Ren, Aliaksandr Siarohin, Bing Li, Hsin-Ying Lee, Ivan Skorokhodov, Peter Wonka, Sergey Tulyakov, et al. Magic123: One image to high-quality 3d object generation using both 2d and 3d diffusion priors. In *ICLR*, 2024. 11
- [46] Lingteng Qiu, Guanying Chen, Xiaodong Gu, Qi Zuo, Mutian Xu, Yushuang Wu, Weihao Yuan, Zilong Dong, Liefeng Bo, and Xiaoguang Han. Richdreamer: A generalizable normal-depth diffusion model for detail richness in text-to-3d. In *CVPR*, 2024. 11
- [47] Alec Radford, Jong Wook Kim, Chris Hallacy, Aditya Ramesh, Gabriel Goh, Sandhini Agarwal, Girish Sastry, Amanda Askell, Pamela Mishkin, Jack Clark, et al. Learning transferable visual models from natural language supervision. In *ICML*, 2021. 11
- [48] Olaf Ronneberger, Philipp Fischer, and Thomas Brox. U-net: Convolutional networks for biomedical image segmentation. In *MICCAI*, 2015. 3
-

- [49] Johannes L Schönberger, Enliang Zheng, Jan-Michael Frahm, and Marc Pollefeys. Pixelwise view selection for unstructured multi-view stereo. In *ECCV*, 2016. 11
- [50] Johannes Lutz Schönberger and Jan-Michael Frahm. Structure-from-motion revisited. In *CVPR*, 2016. 11
- [51] Tianchang Shen, Jun Gao, Kangxue Yin, Ming-Yu Liu, and Sanja Fidler. Deep marching tetrahedra: a hybrid representation for high-resolution 3d shape synthesis. In *NeurIPS*, 2021. 11
- [52] Tianchang Shen, Jacob Munkberg, Jon Hasselgren, Kangxue Yin, Zian Wang, Wenzheng Chen, Zan Gojic, Sanja Fidler, Nicholas Sharp, and Jun Gao. Flexible isosurface extraction for gradient-based mesh optimization. *ACM Transactions on Graphics (TOG)*, 2023. 5, 11
- [53] Ruoxi Shi, Hansheng Chen, Zhuoyang Zhang, Minghua Liu, Chao Xu, Xinyue Wei, Linghao Chen, Chong Zeng, and Hao Su. Zero123++: a single image to consistent multi-view diffusion base model. *arXiv preprint arXiv:2310.15110*, 2023. 11
- [54] Yichun Shi, Peng Wang, Jianglong Ye, Mai Long, Kejie Li, and Xiao Yang. Mvdream: Multi-view diffusion for 3d generation. *arXiv preprint arXiv:2308.16512*, 2023. 2, 11
- [55] Noah Snavely, Steven M Seitz, and Richard Szeliski. Photo tourism: exploring photo collections in 3d. *ACM Transactions on Graphics (TOG)*, 2006. 11
- [56] Yang Song and Stefano Ermon. Generative modeling by estimating gradients of the data distribution. In *NeurIPS*, 2019. 2
- [57] Jingxiang Sun, Bo Zhang, Ruizhi Shao, Lizhen Wang, Wen Liu, Zhenda Xie, and Yebin Liu. Dreamcraft3d: Hierarchical 3d generation with bootstrapped diffusion prior. In *ICLR*, 2024. 11
- [58] Jiaxiang Tang, Jiawei Ren, Hang Zhou, Ziwei Liu, and Gang Zeng. Dreamgaussian: Generative gaussian splatting for efficient 3d content creation. *arXiv preprint arXiv:2309.16653*, 2023. 11
- [59] Junshu Tang, Tengfei Wang, Bo Zhang, Ting Zhang, Ran Yi, Lizhuang Ma, and Dong Chen. Make-it-3d: High-fidelity 3d creation from a single image with diffusion prior. In *ICCV*, 2023. 11
- [60] Shitao Tang, Jiacheng Chen, Dilin Wang, Chengzhou Tang, Fuyang Zhang, Yuchen Fan, Vikas Chandra, Yasutaka Furukawa, and Rakesh Ranjan. Mvdifusion++: A dense high-resolution multi-view diffusion model for single or sparse-view 3d object reconstruction. *arXiv preprint arXiv:2402.12712*, 2024. 11
- [61] Ashish Vaswani, Noam Shazeer, Niki Parmar, Jakob Uszkoreit, Llion Jones, Aidan N Gomez, Łukasz Kaiser, and Illia Polosukhin. Attention is all you need. In *NeurIPS*, 2017. 2, 11
- [62] Haochen Wang, Xiaodan Du, Jiahao Li, Raymond A Yeh, and Greg Shakhnarovich. Score jacobian chaining: Lifting pretrained 2d diffusion models for 3d generation. In *CVPR*, 2023. 11
- [63] Peng Wang and Yichun Shi. Imagedream: Image-prompt multi-view diffusion for 3d generation. *arXiv preprint arXiv:2312.02201*, 2023. 11
- [64] Peng Wang, Lingjie Liu, Yuan Liu, Christian Theobalt, Taku Komura, and Wenping Wang. Neus: Learning neural implicit surfaces by volume rendering for multi-view reconstruction. In *NeurIPS*, 2021. 4, 11
- [65] Zhengyi Wang, Cheng Lu, Yikai Wang, Fan Bao, Chongxuan Li, Hang Su, and Jun Zhu. Prolificdreamer: High-fidelity and diverse text-to-3d generation with variational score distillation. In *NeurIPS*, 2024. 11

- [66] Haohan Weng, Tianyu Yang, Jianan Wang, Yu Li, Tong Zhang, CL Chen, and Lei Zhang. Consistent123: Improve consistency for one image to 3d object synthesis. *arXiv preprint arXiv:2310.08092*, 2023. [11](#)
- [67] Kevin Xie, Jonathan Lorraine, Tianshi Cao, Jun Gao, James Lucas, Antonio Torralba, Sanja Fidler, and Xiaohui Zeng. Latte3d: Large-scale amortized text-to-enhanced3d synthesis. *arXiv preprint arXiv:2403.15385*, 2024. [11](#)
- [68] Xudong Xu, Zhaoyang Lyu, Xingang Pan, and Bo Dai. Matlaber: Material-aware text-to-3d via latent brdf auto-encoder. *arXiv preprint arXiv:2308.09278*, 2023. [11](#)
- [69] Jiayu Yang, Ziang Cheng, Yunfei Duan, Pan Ji, and Hongdong Li. Consistnet: Enforcing 3d consistency for multi-view images diffusion. In *CVPR*, 2024. [11](#)
- [70] Lior Yariv, Jiatao Gu, Yoni Kasten, and Yaron Lipman. Volume rendering of neural implicit surfaces. In *NeurIPS*, 2021. [5](#), [6](#), [11](#)
- [71] Taoran Yi, Jiemin Fang, Guanjun Wu, Lingxi Xie, Xiaopeng Zhang, Wenyu Liu, Qi Tian, and Xingang Wang. Gaussiandreamer: Fast generation from text to 3d gaussian splatting with point cloud priors. *arXiv preprint arXiv:2310.08529*, 2023. [11](#)
- [72] Wangbo Yu, Li Yuan, Yan-Pei Cao, Xiangjun Gao, Xiaoyu Li, Long Quan, Ying Shan, and Yonghong Tian. Hifi-123: Towards high-fidelity one image to 3d content generation. *arXiv preprint arXiv:2310.06744*, 2023. [11](#)
- [73] Xiaohui Zeng, Arash Vahdat, Francis Williams, Zan Gojcic, Or Litany, Sanja Fidler, and Karsten Kreis. Lion: Latent point diffusion models for 3d shape generation. In *NeurIPS*, 2022. [11](#)
- [74] Lvmin Zhang, Anyi Rao, and Maneesh Agrawala. Adding conditional control to text-to-image diffusion models. In *ICCV*, 2023. [2](#), [3](#)
- [75] Richard Zhang, Phillip Isola, Alexei A Efros, Eli Shechtman, and Oliver Wang. The unreasonable effectiveness of deep features as a perceptual metric. In *CVPR*, 2018. [6](#)
- [76] Xiuming Zhang, Pratul P Srinivasan, Boyang Deng, Paul Debevec, William T Freeman, and Jonathan T Barron. Nerfactor: Neural factorization of shape and reflectance under an unknown illumination. *ACM Transactions on Graphics (ToG)*, 2021. [11](#)
- [77] Joseph Zhu and Peiye Zhuang. Hifa: High-fidelity textto-3d with advanced diffusion guidance. *arXiv preprint arXiv:2305.18766*, 2023. [11](#)